ON THE ANALYSIS OF VISCOPLASTIC BUCKLING

LARS PILGAARD MIKKELSEN

Department of Solid Mechanics, The Technical University of Denmark, DK 2800, Lyngby,
Denmark

Abstract—For elastic–viscoplastic structures the classical elastic–plastic bifurcation approach to inelastic buckling is not valid. Only an elastic bifurcation point exists in the elastic–viscoplastic case, and the inelastic buckling behaviour is controlled by a strong sensitivity to small imperfections. However, in the last few years some papers have been published on an approximation that leads to a so-called viscoplastic bifurcation point. Results of accurate numerical analyses for elastic–viscoplastic columns are compared with predictions based on the approximate bifurcation approach. In some cases the bifurcation approach gives a poor approximation of the actual elastic–viscoplastic column behaviour, whereas in other cases the discrepancy is less pronounced. The simple column model gives a clear illustration of the effect, but similar results for plates are also mentioned briefly.

1. INTRODUCTION

For classical time-independent elastic–plastic material behaviour the buckling of column, plate, and shell structures in the plastic range is governed by Hill's (1958) general theory of bifurcation and uniqueness in elastic–plastic solids.

Experimental measurements show that even at low strain-rate, the inelastic behaviour of metals tends to be viscoplastic such that the flow stress is dependent on the strain-rate. According to Hill's bifurcation theory it can be shown that the plastic bifurcation point vanishes in the viscoplastic case. However, numerical computations for structures with small initial imperfections and rather little strain-rate sensitivity have shown that the maximum support load is usually close to the critical bifurcation point for the corresponding time-independent plastic solid. The explanation seems to be that the central role played by the critical plastic bifurcation point in the case of time-independent elastic–plastic material behaviour is replaced by a strong sensitivity to small initial imperfections (Tvergard, 1985). In spite of this, an approximation leading to a so-called viscoplastic bifurcation load (here called a BNM-load) has been suggested by Bodner *et al.* (1991) and used by Paley and Aboudi (1991a, b). The BNM-analysis has the advantage over a full numerical analysis that it gives a quick estimate of the buckling load.

In the present paper a comparison is made between the approximate BNM-load and the maximum support load found by an accurate numerical analysis for imperfect elastic–viscoplastic structures. The study is concentrated on a simple-supported column with a solid rectangular cross-section under axial compression, which gives a clear illustration of the effect; but some similar results for a column with a T-cross-section and for a simply-supported plate under axial compression are also mentioned briefly. The statement of Bodner *et al.* (1991) that the BNM-load provides a lower bound to the buckling load is discussed on the basis of this comparison.

The numerical results for the columns are calculated using an incremental finite element method in which the displacement components are approximated by Hermitian cubics. The viscoplastic constitutive law is chosen to be identical to that used by Tvergaard (1985), and the usual non-linear Bernoulli–Euler beam theory is applied. The plate results are based on an analogous approximation in the context of von Karman plate theory [see e.g. Tvergaard (1987)].

2. BASIC EQUATIONS

It is assumed here that the conditions for small strain theory are satisfied, and the material is assumed to be isotropic hardening. Following the description given by Tvergaard

(1985) the total strain-rate $\dot{\eta}_{ij}$ is taken to be the sum of an elastic part $\dot{\eta}_{ij}^{E}$, and a viscoplastic part $\dot{\eta}_{ij}^{P}$:

$$\dot{\eta}_{ij} = \dot{\eta}_{ij}^{E} + \dot{\eta}_{ij}^{P}, \tag{1}$$

where (˙) denotes the time derivative. Cartesian tensor notation is used, where ( )$_{,i}$ denotes partial differentiation in the reference frame, Latin and Greek indices range from one to three and from one to two, respectively, and the summation convention is adopted for repeated indices [see e.g. Niordson (1985)].

The elastic part $\dot{\eta}_{ij}^{E}$ is taken to follow the time-independent generalized Hooke's law. The viscoplastic part is modelled by a power-law variation of the effective plastic strain-rate $\dot{\varepsilon}_{e}^{P}$:

$$\dot{\varepsilon}_{e}^{P} = \dot{\varepsilon}_{0} \left(\frac{\sigma_{e}}{g(\varepsilon_{e}^{P})} \right)^{1/m}. \tag{2}$$

Here, $\sigma_{e} = \sqrt{3s_{ij}s_{ij}/2}$ is the effective von Mises stress, with the stress deviator $s_{ij} = \sigma_{ij} - \delta_{ij}\sigma_{kk}/3$, δ_{ij} is Kronecker's delta, m is the rate-hardening exponent, and $\dot{\varepsilon}_{e}^{P} = \sqrt{2\dot{\eta}_{ij}^{P}\dot{\eta}_{ij}^{P}/3}$. Furthermore, $\dot{\varepsilon}_{0}$ is a positive reference strain-rate, such that the function $g(\varepsilon_{e}^{P})$ represents the flow stress in a uniaxial tensile test performed at a strain-rate corresponding to $\dot{\varepsilon}_{e}^{P} = \dot{\varepsilon}_{0}$. The uniaxial stress-strain law is modelled by a piecewise power-law with continuous tangent modulus, such that the connection between ε_{e}^{P} and $g(\varepsilon_{e}^{P})$ is:

$$\varepsilon_{e}^{P} = \frac{\sigma_{0}}{E} \left[\frac{1}{n} \left(\frac{g(\varepsilon_{e}^{P})}{\sigma_{0}} \right)^{n} - \frac{1}{n} + 1 \right] - \frac{g(\varepsilon_{e}^{P})}{E}, \tag{3}$$

where $g(0) = \sigma_{0}$. Here, σ_{0} is the reference yield stress, n the strain hardening exponent, and E is Young's modulus. The direction of the plastic part of the strain-rate tensor is taken to be normal to a potential surface proportional to the von Mises yield surface

$$\dot{\eta}_{ij}^{P} = \dot{\varepsilon}_{e}^{P} \left(\frac{3}{2} \frac{s_{ij}}{\sigma_{e}} \right). \tag{4}$$

The concept of elastic unloading is not directly incorporated in the viscoplastic model, but in cases where the value of the rate-hardening exponent m in (2) is small (note that $m \approx 1\text{-}2 \cdot 10^{-2}$ for steel at room temperature), unloading is effectively represented by (2). Then, the plastic strain-rate is extremely small for σ_{e} slightly smaller than $g(\varepsilon_{e}^{P})$, while the plastic strain-rate is large for $\sigma_{e} > g(\varepsilon_{e}^{P})$, and in the limit $m \to 0$ the present viscoplastic model coincides with the time-independent J_{2}-flow theory.

Now, substituting (1) in Hooke's law, it follows that the elastic-viscoplastic constitutive relations can be written as

$$\dot{\sigma}_{ij} = \mathscr{L}_{ijkl}\dot{\eta}_{kl} + \dot{\sigma}_{ij}^{*}, \quad \dot{\sigma}_{ij}^{*} = -\mathscr{L}_{ijkl}\dot{\eta}_{kl}^{P}, \tag{5}$$

where $\mathscr{L}_{ijkl}$ is the elastic modulus given by

$$\mathscr{L}_{ijkl} = \frac{E}{1+v} \left\{ \frac{1}{2}(\delta_{ik}\delta_{jl} + \delta_{il}\delta_{jk}) + \frac{v}{1-2v}\delta_{ij}\delta_{kl} \right\} \tag{6}$$

and v is Poisson's ratio.

3. BERNOULLI–EULER COLUMNS

In the analyses to be presented here, it is assumed that the non-linear Bernoulli–Euler beam theory with a uniaxial state of stress is sufficient [see e.g. Tvergaard (1985) and Hutchinson (1974)]. The x^1- and x^3-axes are chosen along the centreline and normal to the centreline, respectively, and the corresponding displacements are denoted by v and w. If the strain-rate component $\dot{\eta}_{11}$ in the x^1-direction is denoted $\dot{\eta}$, then $\dot{\eta}$ can be written as

$$\dot{\eta} = \dot{\varepsilon} - x^3 \dot{\kappa}, \tag{7}$$

where $\dot{\varepsilon}$ is the strain-rate of the centreline and $\dot{\kappa}$ the bending strain-rate, given by

$$\dot{\varepsilon} = v_{,1} + w_{,1} \dot{w}_{,1}, \quad \dot{\kappa} = \dot{w}_{,11}. \tag{8}$$

With $\dot{\sigma} = \dot{\sigma}_{11}$ the rates of the axial force N and the bending moment M are

$$\dot{N} = \int_A \dot{\sigma} \, \mathrm{d}A, \quad \dot{M} = -\int_A \dot{\sigma} x^3 \, \mathrm{d}A, \tag{9}$$

where A is the area of the column cross-section. Then, the one-dimensional version of the constitutive equation (5) leads to the constitutive relations for the column:

$$\dot{N} = H^{(1)}\dot{\varepsilon} + H^{(2)}\dot{\kappa} + \dot{N}^*,$$
$$\dot{M} = H^{(2)}\dot{\varepsilon} + H^{(3)}\dot{\kappa} + \dot{M}^*, \tag{10}$$

where

$$H^{(i)} = \int_A E(-x^3)^{i-1} \, \mathrm{d}A, \quad \dot{N}^* = \int_A \dot{\sigma}^* \, \mathrm{d}A, \quad \dot{M}^* = -\int_A x^3 \dot{\sigma}^* \, \mathrm{d}A, \tag{11}$$

and $\dot{\sigma}^*$ can be written as

$$\dot{\sigma}^* = -E\dot{\eta}^{\mathrm{P}}, \quad \dot{\eta}^{\mathrm{P}} = \dot{\varepsilon}_{\mathrm{e}}^{\mathrm{P}} \frac{\sigma}{\sigma_{\mathrm{e}}}. \tag{12}$$

The principle of virtual work is used to express the requirement of equilibrium for the column:

$$\int_0^a (N\delta\varepsilon + M\delta\kappa) \, \mathrm{d}x^1 = \delta W, \tag{13}$$

where a is the length of the column and δW is the external virtual work. The numerical results are found by a linear incremental method, based on the incremental principle of virtual work

$$\Delta t \int_0^a (\dot{N}\delta\varepsilon + \dot{M}\delta\kappa + N\dot{w}\delta w) \, \mathrm{d}x^1 = \Delta t \delta\dot{W} - \left[\int_0^a (N\delta\varepsilon + M\delta\kappa) \, \mathrm{d}x^1 - \delta W \right]. \tag{14}$$

Here, the bracketed terms are included to avoid drifting away from the equilibrium path.

4. BIFURCATION THEORY

Hill's (1958) general theory of uniqueness and bifurcation, has been used with great success in the analysis of buckling of time-independent elastic–plastic solids [see e.g. Hutchinson (1974)]. For a column, the expression used by Hill to prove uniqueness can be written as

$$I = \int_{0}^{a} (\tilde{N}\tilde{\varepsilon} + \tilde{M}\tilde{\kappa} + N^{0}\tilde{w}\tilde{w})\,dx^{1}. \tag{15}$$

Here, $(\ )^{0}$ denotes the fundamental solution and $(\tilde{\ }) = (\cdot)^{a} - (\cdot)^{b}$ is defined as the difference between two distinct incremental solutions, to the incremental principle of virtual work (14) for a given prescribed load or displacement increment. The lowest critical bifurcation point is reached when (15) has a non-trivial solution $(\tilde{\ })$.

Expression (15) can also be used in the viscoplastic case. Here, the plastic part $\dot{\eta}^{p}$ of the strain-rate is directly a function of the current state of stress and strain, and does not depend on the rates (2). Therefore, at any prescribed load increment it is seen that $\tilde{\dot{\eta}}^{p} \equiv 0$, since the states of stress and strain are known, and thus $\tilde{\dot{\eta}} = \tilde{\dot{\eta}}^{E}$. It follows that (15) only gives an elastic bifurcation point [see Obrecht (1977) and Tvergaard (1989)]. The numerical analyses to be presented here in Section 5 and that presented by Tvergaard (1985) show that the maximum support load for a viscoplastic column is at most $1.2\lambda_{cp}$ (for the rate-hardening exponent $m = 0.05$ and the speed of the average axial shortening $\dot{\varepsilon}_{a} \leqslant 10\dot{\varepsilon}_{0}$), even for columns with an initial imperfection as small as $\bar{\xi} = 10^{-7}$. Here, λ_{cp} is the critical bifurcation load for the corresponding time-independent plastic solid. The elastic bifurcation load λ_{ce} is in these examples much higher than λ_{cp}, $2.18 < \lambda_{ce}/\lambda_{cp} < 2.93$, and the maximum support load is therefore far below the critical bifurcation load λ_{ce} for the viscoplastic material. The only explanation seems to be that the governing effect of the plastic bifurcation point for time-independent elastic–plastic solids is replaced by a strong sensitivity to small initial imperfections in the case of the elastic–viscoplastic solids [see also Tvergaard (1991)].

In spite of this, Bodner et al. (1991) have suggested an approximation method which gives a "viscoplastic bifurcation point". The idea of this approximation is that the plastic strain-rate $\dot{\varepsilon}_{e}^{p}$ is held constant during differentiation of the viscoplastic constitutive law (2), with respect to the plastic strain ε_{e}^{p}. It is then possible to define an inelastic tangent modulus $E_{t}^{p} = d\sigma_{e}/d\varepsilon_{e}^{p}$. With the viscoplastic constitutive law (2) presented in Section 2 the following expression is obtained:

$$E_{t}^{p} = \frac{d\sigma_{e}}{d\varepsilon_{e}^{p}}\bigg|_{\dot{\varepsilon}_{e}^{p} = \text{const.}} = \left(\frac{\dot{\varepsilon}_{e}^{p}}{\dot{\varepsilon}_{0}}\right)\frac{dg(\varepsilon_{e}^{p})}{d\varepsilon_{e}^{p}}, \tag{16}$$

where $dg(\varepsilon_{e}^{p})/d\varepsilon_{e}^{p}$ is obtained from (3):

$$\frac{dg(\varepsilon_{e}^{p})}{d\varepsilon_{e}^{p}} = \frac{E}{\left(\dfrac{g(\varepsilon_{e}^{p})}{\sigma_{0}}\right)^{n-1} - 1}. \tag{17}$$

It is emphasized that, due to the assumptions made, E_{t}^{p} is not a real tangent modulus. However, in the limit of a time-independent elastic–plastic material the connection between E_{t}^{p} and the total tangent modulus E_{t} would be given by

$$E_{t} = \frac{E_{t}^{p}}{1 + \dfrac{E_{t}^{p}}{E}}. \tag{18}$$

In the BNM-approximation Hill's bifurcation theory for time-independent elastic–

plastic solids is then used with the time-independent tangent modulus E_t replaced by the modulus (18). Thus a "viscoplastic bifurcation point" is found. In the following this point is called a BNM-point. In the time-independent limit the BNM-point coincides with the time-independent plastic bifurcation point λ_{cp} [see Tvergaard (1991)].

5. NUMERICAL RESULTS

The following numerical results are found for a simply-supported column with a solid rectangular cross-section. The rectangular cross-section has the thickness h and the width b, where $b > h$, and the column length is a. For time-independent plasticity a column of this type has the critical bifurcation point

$$\lambda_{cp} P = \left(\frac{\pi}{a}\right)^2 E_t^c I \tag{19}$$

and the corresponding critical bifurcation mode

$$w^{(1)} = h \sin\left(\frac{\pi x^1}{a}\right), \quad v^{(1)} \equiv 0. \tag{20}$$

Here, P is a constant compressive axial load, λ_{cp} is a positive load parameter, I is the area moment of inertia of the cross-section, and E_t^c is the tangent modulus at bifurcation. The axial displacement rate $\dot{v}(a) = a\dot{\varepsilon}_a$ at the end of the column is prescribed, where $\dot{\varepsilon}_a$ represents the average axial strain-rate in the column.

The present full numerical analyses are carried out for an imperfect column with an initial imperfection $\bar{w} = \bar{\xi} w^{(1)}$. This is the most critical imperfection mode in the time-independent limit for a sufficiently small $\bar{\xi}$.

The analysis is based on an incremental finite element method, where the displacement rates $\dot{v}$ and $\dot{w}$ are approximated by Hermitian cubics. It has been found that it is sufficient to use two elements over the half-length of the column, with a three-point Gauss quadrature to evaluate (14) in each element and a seven-point Simpson integration to evaluate (11). This has been shown by comparison with a few numerical calculations for four or six elements over the half-length and for four-point Gauss quadrature.

In the following figures all the loads are normalized with respect to the lowest critical bifurcation load λ_{cp} found for the corresponding J_2-flow theory. Here, λ_{ce} and λ_{cp} are the elastic and the plastic bifurcation load parameters, respectively, and $\lambda_c = \min\{\lambda_{ce}, \lambda_{cp}\}$.

In the following, numerical results are shown for a column with a strain hardening exponent $n = 10$, and a ratio $\sigma_{cp}/\sigma_0 = 1.11$ between the lowest critical compressive bifurcation stress for time-independent J_2-flow theory, and the reference stress. This corresponds to a ratio $\lambda_{ce}/\lambda_{cp} = E/E_t^c = 2.66$ between the time-independent elastic and plastic bifurcation loads. Numerical results are shown for different initial imperfections $\bar{\xi}$, and for different rate-hardening exponents m.

Figure 1 shows the load versus the mode amplitude ξ for a column, where the prescribed displacement rate of the column end is given by $\dot{\varepsilon}_a = \dot{\varepsilon}_0$. The amplitude ξ specifies the
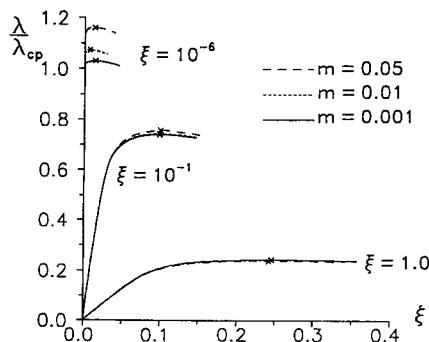

Fig. 1. Load versus bifurcation mode amplitude for a column with $\sigma_{cp}/\sigma_0 = 1.11$, $n = 10$ and $\dot{\varepsilon}_a = \dot{\varepsilon}_0$.
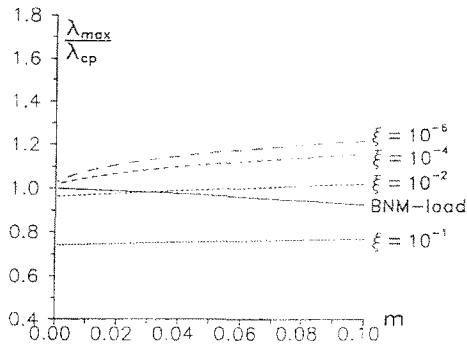
Fig. 2. Load versus rate-hardening exponent m for a column with $\sigma_{cp}/\sigma_0 = 1.11$, $n = 10$ and $\dot{\varepsilon}_a = \dot{\varepsilon}_0$.

deflection at the centre of the column, in addition to the initial imperfection amplitude $\bar{\xi}$. The load carrying capacity of the column is seen to have the greatest sensitivity to the rate-hardening exponent m when the initial imperfection $\bar{\xi}$ is small. This was also found by Tvergaard (1985).

Figure 2 shows the maximum support load for a whole spectrum of rate-hardening exponents $m \in [0.001 ; 0.10]$. This is shown for columns with four different initial imperfections $\bar{\xi}$. The corresponding "viscoplastic bifurcation load" predicted by the BNM-approach is shown in the same figure, so that it is possible to evaluate the usefulness of the BNM-load as an approach to predicting the load-carrying capacity of the viscoplastic column. The bifurcation load λ_{cp} for the corresponding time-independent elastic–plastic column is one possibility of a quick estimate of the load-carrying capacity, which is independent of $\dot{\varepsilon}_a$ and m. The BNM-load gives a better quick estimate, if the dependence on these parameters is better described, by comparing it with the actual maximum support load for the imperfect viscoplastic column. In the time-independent limit ($m \to 0$) it is seen that the plastic bifurcation load is practically identical to the maximum support load when the imperfection is small, as expected [e.g. Tvergaard and Needlemann (1977)]. For a viscoplastic material with a larger rate-hardening exponent m an increasing difference between the maximum support load for columns with small initial imperfection $\bar{\xi}$ and the BNM-approach is seen. It is even seen that the BNM-load is decreasing for increasing m-value, in spite of the fact that the maximum support load is increasing. A comparison of the critical bifurcation load λ_{cp} for the corresponding time-independent column and the BNM-load as it approaches a quick estimate of the load-carrying capacity of the viscoplastic column it is seen in this case that λ_{cp} gives a better description of the m-dependence than the BNM-load.

A change in the average axial strain-rate $\dot{\varepsilon}_a$ has a significant effect on the variation with m of the maximum support load and the BNM-load, but has only a small effect on the deviation between the loads. The BNM-load and the maximum support load change to higher or lower values when the axial strain-rate is increased or decreased, respectively. The difference between the maximum support load and the BNM-load seen in Fig. 2 is therefore not altered significantly with a change in the prescribed average strain-rate $\dot{\varepsilon}_a$. This can be seen by comparing Fig. 2 with Figs 3 and 4, where the axial strain-rate $\dot{\varepsilon}_a$ is as small as $\dot{\varepsilon}_a = \dot{\varepsilon}_0/100$, and as large as $\dot{\varepsilon}_a = 100\dot{\varepsilon}_0$, but in these two figures the BNM-load gives a better description of the m-dependence than λ_{cp}. Here, and in all other cases, it is assumed that the displacement rate in the column is such that inertia effects are negligible.

For comparison with Fig. 2, Fig. 5 shows the effect of a change in the strain hardening exponent n. The n-value is here changed to $n = 100$. This corresponds to $\sigma_{cp}/\sigma_0 = 1.01$ and $\lambda_{ce}/\lambda_{cp} = 2.93$. It is seen that the agreement of the BNM-load with the real maximum support load of the viscoplastic column is not as good for $n = 100$ (Fig. 5) than found for $n = 10$ (Fig. 2).

Figure 6 shows again the maximum support load and the corresponding BNM-load, but contrary to Figs 2–5, where the loads are plotted against the rate-hardening exponent m, the loads in Fig. 6 are plotted against the ratio between the critical bifurcation stress σ_c
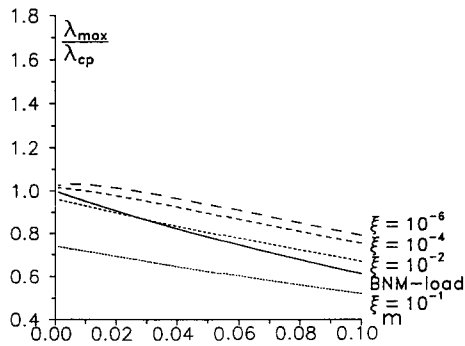
Fig. 3. Load versus rate-hardening exponent m for a column with $\sigma_{cp}/\sigma_0 = 1.11$, $n = 10$ and
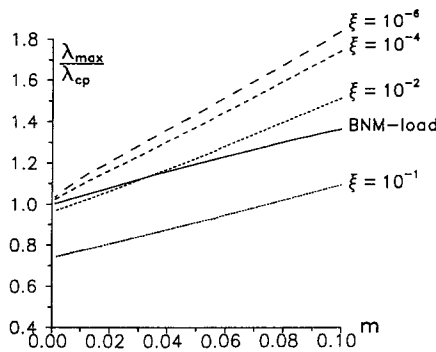$$\dot{\varepsilon}_a = \dot{\varepsilon}_0/100.$$

Fig. 4. Load versus rate-hardening exponent m for a column with $\sigma_{cp}/\sigma_0 = 1.11$, $n = 10$ and
$$\dot{\varepsilon}_a = 100\dot{\varepsilon}_0.$$

for the corresponding time-independent elastic–plastic material and the reference stress σ_0, where a low value of σ_c/σ_0 corresponds to a relatively thin column (for a given value of σ_0) while a higher value of σ_c/σ_0 corresponds to a thicker column. This is one way of presenting the column load-carrying capacity that is also used by Hutchinson (1974) for the time-independent case. The loads are normalized by the lowest bifurcation load for the time-independent elastic–plastic material, i.e. the elastic bifurcation load $\lambda_{ce} = (\pi/a)^2 EI$ for $\sigma_c < \sigma_0$ and the plastic bifurcation load $\lambda_{cp} = (\pi/a)^2 E_t^c I$ [see eqn (19)] for $\sigma_c > \sigma_0$. It is the change from the elastic to the plastic bifurcation load that causes the kink on the curves at $\sigma_c = \sigma_0$. Figure 6 shows columns where σ_c/σ_0 varies from 0.32 (thin column) to 1.22 (thick column). The upper half of the figure shows the maximum support load for three different m-values and three different initial imperfections $\bar{\xi}$. The corresponding BNM-loads for the same three m-values are presented in the lower half of the figure. The value of the strain hardening exponent is $n = 10$ and the prescribed average strain-rate is $\dot{\varepsilon}_a = \dot{\varepsilon}_0$.
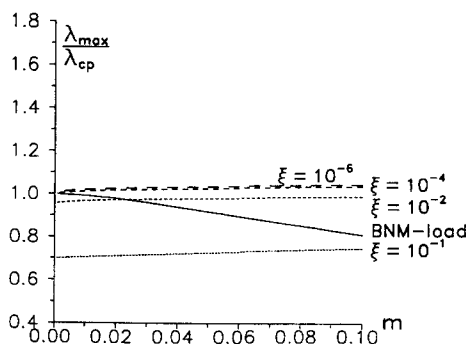

Fig. 5. Load versus rate-hardening exponent m for a column with $\sigma_{cp}/\sigma_0 = 1.01$, $n = 100$ and $\dot{\varepsilon}_a = \dot{\varepsilon}_0$.
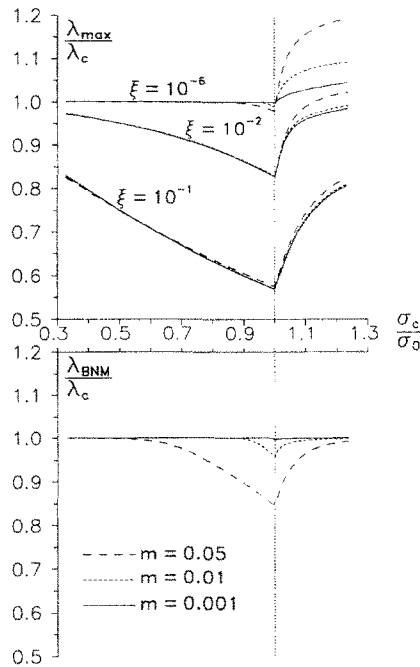
Fig. 6. Maximum supported load and BNM-load versus critical bifurcation stress for a column with
$n = 10$, and $\dot{\varepsilon}_a = \dot{\varepsilon}_0$, when the column thickness is varied so that σ_c/σ_0 varies.

It is seen in Fig. 6 that the maximum support load is most imperfection sensitive when $\sigma_c \approx \sigma_0$. The sensitivity to the rate-hardening exponent m is very small for $\sigma_c/\sigma_0 < 1$, but increases when σ_c/σ_0 exceeds unity and when $\bar{\xi}$ is decreasing. For σ_c/σ_0 above unity and for a small $\bar{\xi}$, it is seen that the maximum support load increases with an increasing m-value.

Contrary to this the BNM-load is seen to have the greatest sensitivity to the rate-hardening exponent m when σ_c/σ_0 is around unity, and the BNM-load is seen to decrease with an increasing m-value. In addition to this the BNM-load is also seen to have a significant sensitivity to the rate-hardening exponent when $\sigma_c < \sigma_0$, which is not found at all for the maximum support load of the real viscoplastic column. The difference between the sensitivity of the BNM-load and that of the real maximum support load to the m-value when σ_c/σ_0 is around unity agrees with the difference found between Figs 2 and 5, where the higher value of the strain hardening exponent n gives a value of σ_c/σ_0 near unity.

If the plastic part of the average strain-rate is prescribed to be $\dot{\varepsilon}_a^P = \dot{\varepsilon}_0$, instead of prescribing a fixed value of the total average strain-rate $\dot{\varepsilon}_a$ (as in Figs 1–6), it is seen from (16)–(18) that the sensitivity of the BNM-load to the rate-hardening exponent m must vanish as the BNM-load is calculated for perfect structures. The same is not true for the maximum support load of the imperfect column, where the plastic strain-rate is not constant through the column, and in the case of $\dot{\varepsilon}_a^P = \dot{\varepsilon}_0$ a significant m-sensitivity of the maximum support load will therefore be expected. No analysis has been made here for this case, because a complex variation of $\dot{\varepsilon}_a$ would be required.

In comparing the BNM-load with the actual maximum support load of an imperfect viscoplastic column it is important to note that the latter depends on the imperfection amplitude $\bar{\xi}$, while the BNM-load refers to a perfect column. A reasonable comparison is obtained by focusing on the maximum support load for a given small imperfection. It is seen in Fig. 2 that in the time-independent limit ($m \to 0$) the maximum support load for $\bar{\xi} = 10^{-2}$ is about 4% below λ_{cp} while the maximum support load for $\bar{\xi} = 10^{-4}$ is slightly above λ_{cp}. If $\bar{\xi} = 10^{-4}$ is chosen to be compared with the BNM-load it is seen from Fig. 2 that the BNM-load is 5% below the maximum support load when $m = 0.01$ and that the BNM-load is 12% below the maximum support load when $m = 0.05$.

A column with a T-cross-section (Fig. 7) has also been analysed. This structure corresponds to a panel which buckles in a column mode like that analysed by Tvergaard (1985). The column to be re-analysed here has a cross-section defined by:
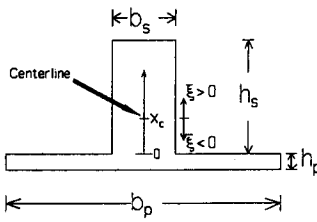
Fig. 7. T-cross-section of a column.

$$\frac{b_s}{a} = 0.0112, \quad \frac{b_p}{a} = 0.2500, \quad \frac{h_s}{a} = 0.0500, \quad \frac{h_p}{a} = 0.00416, \tag{21}$$

where a is the length of the simply-supported column. The material is defined by:

$$\frac{\sigma_0}{E} = 0.001, \quad n = 10. \tag{22}$$

This corresponds to

$$\frac{\lambda_{ce}}{\lambda_{cp}} = \frac{E}{E_t^c} = 2.18, \quad \frac{\sigma_c}{\sigma_0} = 1.09. \tag{23}$$

Again, the initial imperfection is in the shape of the critical bifurcation mode (20), where h is replaced by h_p. Only the most imperfection-sensitive range $\bar{\xi} < 0$ is analysed.

Figure 8 shows a comparison between the maximum support load of the viscoplastic imperfect column and the BNM-load, analogous to Figs 2–5. The imperfection is chosen so that it is possible to compare the maximum support load with the results presented by Tvergaard (1985), and the comparison shows fine agreement. In comparison with the maximum support load for the rectangular cross-section the maximum support load for the T-cross-section shows a greater sensitivity to the value of the rate-hardening exponent m. Comparison between the maximum support load and the BNM-approach gives a picture similar to Fig. 2, with a slightly bigger difference. A change in the average axial strain-rate $\dot{\varepsilon}_a$ is found to have the same sort of effect as that observed for the rectangular cross-section (Figs 3 and 4).

A simply-supported rectangular plate under axial compression, with the edges constrained to remain straight, has also been analysed. The usual first order plate theory is used with a non-linear strain tensor and a linear bending tensor [see Niordson (1985)]. The theory will not be explained here, but more information on plastic plate buckling can be found in Needlemann and Tvergaard (1976) and Hutchinson (1974). The displacement rates
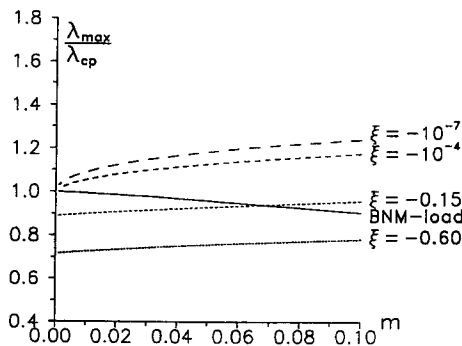

Fig. 8. Load versus rate-hardening exponent m for the column with T-cross-section (21), for $n = 10$ and $\dot{\varepsilon}_a = \dot{\varepsilon}_0$.
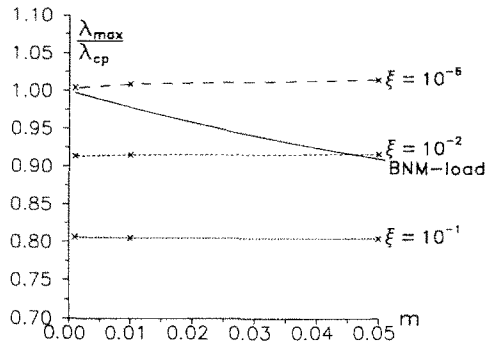
Fig. 9. Load versus m for plate with $b/a = 2$, $h/a = 0.050$, $\sigma_0/E = 0.00337$, $v = 0.3$, $n = 10$ and $\dot{\varepsilon}_a = \dot{\varepsilon}_0$.

$\dot{v}_\alpha$, $\dot{w}$ are determined by a rectangular plate finite element method. The initial imperfection $\bar{w}$ is in the shape of the critical bifurcation mode $w^{(1)}$:

$$\bar{w} = \xi w^{(1)}, \quad w^{(1)} = h \sin \frac{\pi u^1}{a} \sin \frac{\pi u^2}{b}, \tag{24}$$

where h is the thickness, a the length, and b the width of the plate. The corresponding time-independent elastic–plastic bifurcation point is given by

$$\sigma_{cp} = \frac{h^2}{12} \left(\frac{\pi}{a}\right)^2 \left[\frac{E_t}{r-\bar{v}^2} \left(r + 2\bar{v}\left(\frac{a}{b}\right)^2 + \left(\frac{a}{b}\right)^4 \right) + 2\left(\frac{a}{b}\right)^2 \frac{E}{1+\bar{v}} \right],$$

$$\bar{v} = \frac{1}{2} + \frac{E_t}{E}(v-\tfrac{1}{2}), \quad r = \frac{1}{4} + \frac{3}{4}\frac{E_t}{E}. \tag{25}$$

Figure 9 shows the results for a plate with $b/a = 2$, $h/a = 0.05$, $\sigma_0/E = 0.00337$, $v = 0.3$, $n = 10$ and $\dot{\varepsilon}_a = \dot{\varepsilon}_0$. This corresponds to $\sigma_{cp}/\sigma_0 = 1.0095$. Here is found a very slight sensitivity of the maximum support load to the rate-hardening exponent m. By contrast, the BNM-load predicts a significant sensitivity to the m-value.

In other calculations, an even larger m-sensitivity of the BNM-load is seen for a thinner plate where σ_c/σ_0 is closer to unity, even though the m-sensitivity remains small for the actual maxiumum support load. The observation for the column (Figs 2–5) that the change of the BNM-load and the maximum support load is of the same size when the average strain-rate $\dot{\varepsilon}_a$ is changed, is not in general seen for plates. For the plate cases are found where the BNM-load changes very little compared to the maximum support load when the average strain-rate is changed. The BNM-load is identical to λ_{cp} for $m \to 0$ (as in all cases), but the BNM-load does not correctly describe the variation of the structural buckling load with m.

6. DISCUSSION

An evaluation of the BNM-load as an approach to estimating the load-carrying capacity of a viscoplastic column has been presented in this paper. The BNM-load is compared with the real maximum support load found by a full numerical analysis of the imperfect viscoplastic column. This full numerical analysis represents the exact behaviour of the viscoplastic column. A clear evaluation of the BNM-approach is somewhat difficult because it refers to the perfect viscoplastic structure, which does not really have a realistic bifurcation load. The only possible comparison is that with the maximum support load of the imperfect structure, but this load depends on the size of the initial imperfection. As an alternative to the quick estimate obtained by the BNM-load, the critical bifurcation load for the corresponding time-independent plastic material gives another quick estimate,

and it has been found in a number of cases that this alternative estimate gives a better approximation than the BNM-load. Thus, the present analysis of the maximum support load for imperfect viscoplastic structures are applications of well established theories, which are used to obtain an understanding of the usefulness of approximate bifurcation approaches.

It has been stated by Bodner *et al.* (1991) that the BNM-load gives a lower bound to the actual buckling load for the elastic–viscoplastic structure. This is true for the perfect elastic–viscoplastic structure, since only the elastic bifurcation point exists in this case; but the elastic bifurcation load is usually irrelevant, being far above the actual buckling load of the inelastic structure. Clearly, the actual viscoplastic buckling behaviour relies on imperfections or small disturbances. On other hand, the BNM-approach is only defined for the perfect structure.

The BNM-load is also a lower bound of the actual buckling load for a sufficiently small imperfection, since this buckling load tends towards the unrealistic elastic buckling load for exceedingly small imperfections [see Tvergaard (1985)]. However, if $\bar{\xi} = 10^{-2}$ is considered to be the smallest realistic imperfection, the present results for columns and plates show that the BNM-load is not always a lower bound. Other results for plates and shells (Mikkelsen, 1992), have shown that even for $\bar{\xi} = 10^{-4}$ the BNM-load is not always a lower bound.

Comparing the BNM-load and the load-carrying capacity of a column with a very small initial imperfection amplitude $\bar{\xi} = 10^{-4}$, it is seen that both loads are very near the critical bifurcation load in the time-independent case, while for $m = 0.01$ the BNM-load is about 5% lower than the maximum support load and for $m = 0.05$ it is about 12% lower.

A change of the rate-hardening exponent is in some cases found to have the opposite effect on the BNM-load than that predicted for the maximum support load, such that one of the loads increases while the other decreases for increasing m-value. At the same time the BNM-load shows most sensitivity to the m-value when the critical stress is around the reference stress, whereas the real load-carrying capacity of the imperfect viscoplastic column shows an increasing sensitivity to the m-value when the critical stress is increased above the reference stress.

A change in the average axial strain-rate has only a small effect on the deviation between the BNM-load and the maximum support load for a column. The BNM-load follows the maximum load of the imperfect column to higher or lower values when the axial strain-rate is increased or decreased, respectively. However, this is not in general found to be true for a simply-supported plate.

REFERENCES

Bodner, S. R., Naveh, M. and Merzer, M. (1991). Deformation and buckling of axisymmetric viscoplastic shells under thermomechanical loading. *Int. J. Solids Structures* **27**, 1915–1924.

Hill, R. (1958). A general theory of uniqueness and stability in elastic–plastic solids. *J. Mech. Phys. Solids* **6**, 236–249.

Hutchinson, J. W. (1974). Plastic buckling. *Advan. Appl. Mech.* **14**, 67–144.

Mikkelsen, L. P. (1992). Viscoplastic buckling of columns, plates and shells (in Danish). Dept. of Solid Mech., Technical University of Denmark.

Needleman, A. and Tvergaard, V. (1976). An analysis of the imperfection sensitivity of square elastic–plastic plates under axial compression. *Int. J. Solids Structures* **12**, 185–201.

Niordson, F. I. (1985). *Shell Theory.* North-Holland series in Applied Mathematics and Mechanics, Vol. 29.

Obecht, H. (1977). Creep buckling and postbuckling of circular cylindrical shells under axial compression. *Int. J. Solids Structures* **13**, 337–355.

Paley, M. and Aboudi, J. (1991a). Viscoplastic bifurcation buckling of plates. *AIAA Jl* **29**, 627–632.

Paley, M. and Aboudi, J. (1991b). Plastic buckling of metal matrix laminated plates. *Int. J. Solids Structures* **28**, 1139–1154.

Tvergaard, V. (1985). Rate-sensitivity in elastic–plastic panel buckling. In *Aspects of the Analysis of Plate Structures, A Volume in Honour of W. H. Wittrick* (Edited by D. J. Dawe, R. W. Horsington, A. G. Kamtekar and G. H. Little), pp. 293–308. Clarendon Press, Oxford.

Tvergaard, V. (1987). Effect of plasticity on post-buckling behaviour. In *Buckling and Postbuckling* (Edited by J. Arbocz, M. Potier-Ferry, J. Singer and V. Tvergaard), pp. 143–183. Springer, Berlin.

Tvergaard, V. (1989). Plasticity and creep at finite strains. In *Theoretical and Applied Mechanics* (Edited by P. Germain, M. Piau and D. Caillerie), pp. 349–368. Elsevier, Amsterdam.

Tvergaard, V. (1991). Tensile instabilities at large strains. Lecture notes from CISM, Udine, Italy (to appear).

Tvergaard, V. and Needleman, A. (1977). On the buckling of elastic–plastic columns with asymmetric cross-section. *Int. J. Mech. Sci.* **17**, 419–424.